Malenov, D. P.; Zarić, S. Stacking Interactions between Ruthenium: P -Cymene Complexes: Combined Crystallographic and Density Functional Study. *CrystEngComm* **2019**, *21* (47), 7204–7210. https://doi.org/10.1039/c9ce01290g

Stacking interactions between ruthenium *p*-cymene complexes. Combined crystallographic and density functional study.

Received 00th January 20xx,
Accepted 00th January 20xx

DOI: 10.1039/x0xx00000x

Dušan P. Malenov[a] and Snežana D. Zarić *[a, b]

The Cambridge Structural Database search for stacking interactions between *p*-cymene (1-methyl-4-isopropylbenzene) ligands of transition metal (mostly ruthenium) complexes revealed three preferred interaction geometries, all with antiparallel orientation. The most frequent one involves both stacking of aromatic rings and C-H/π interactions of methyl substituents with aromatic rings, while the second most frequent has stacking of aromatic rings and C-H/π interactions of methyl groups of isopropyl substituents with aromatic rings. The results of CSD search are in agreement with DFT calculations of interaction energies, since all the preferred CSD geometries correspond to minima on potential energy curves. The strongest calculated interaction between *p*-cymene ligands of model complexes [Ru(*p*-cym)Cl_2(NH_3)] corresponds to the most frequent geometry found in crystal structures, and it has the B97-D2/def2-TZVP interaction energy of -7.56 kcal/mol. This is significantly stronger than interaction between benzene ligands of [Ru(benzene)Cl_2(NH_3)] complexes (-3.93 kcal/mol), revealing that substituents increase interaction strength substantially. All interaction geometries and their relative strengths are in agreement with electrostatic potentials of the monomer complex.

Introduction

Stacking interactions are omnipresent in many chemical and biological systems.[1,2] They stabilize structures of nucleic acids[3,4] and modulate the structure of proteins,[5,6] but they are also important in the fields of materials science,[2] crystal engineering[7,8] and drug design.[9] Although they are usually related to aromatic moieties,[10–12] they can also be very important in the systems containing nonaromatic systems, most notably hydrogen-bridged rings[13] and metal-chelate rings,[8,14] where they can be significantly modulated by the metals in terms of both geometry and energy.[15,16]

Another way for metals to modulate the stacking interactions of aromatic compounds is by the means of coordination to their π-electrons (η-coordination). It was determined that stacking interactions between coordinated and uncoordinated (-4.40 kcal/mol),[17,18] as well as between two coordinated benzenes (-4.01 kcal/mol)[18,19] are stronger than stacking between two uncoordinated benzenes (-2.73 kcal/mol).[10] Stacking interactions of coordinated cyclopentadienyl (Cp) anions are also stronger than stacking between uncoordinated benzenes.[18,20] The searches of Cambridge Structural Database crystal structures revealed the dominance of strong (up to -2.95 kcal/mol)[18,19] stacking interactions at large offsets (more than 4.5 Å) for sandwich compounds, while significantly weaker stacking at large offset of half-sandwich compounds can also be very frequent if it is supported by simultaneous interactions of other ligands of half-sandwich compounds.[18]

Stacking interactions of aromatic rings are in all cases strengthened by the presence of substituents on aromatic rings, regardless of the substituent types.[21–24] This is ascribed to local, direct interactions of substituents of one ring with the closest part of the other aromatic ring, with substituent effects being additive and transferrable.[23]

The topic of this work are stacking interactions between *p*-cymene (1-methyl-4-isopropylbenzene) molecules coordinated to transition metals. Transition metal (mostly ruthenium) complexes that have *p*-cymene ligands are among the very important metal-arene complexes in the field of medicinal chemistry.[25–29] Moreover, they were shown to have certain catalytic activity.[27,30] Apart from that, since *p*-cymene is substituted benzene, it is a good model system to study the influence of substituents on stacking interactions of coordinated aromatic molecules.

In this work we have performed the search of Cambridge Structural Database crystal structures in order to find stacking interactions between two *p*-cymene ligands and to describe their preferred geometries. We have also performed quantum chemical calculations in order to determine the strength of these interactions, as well as to assess the influence of substituents on interaction energies. To the best of our knowledge, this is the first study on stacking interactions between substituted aromatic ligands with η-coordination to transition metals.

Methodology

Cambridge Structural Database (v. 5.40, November 2018)[31] was searched using the ConQuest (v. 2.0.2)[32] program in order to find stacking interactions between *p*-cymene ligands of transition metal complexes. The search included only the crystal structures with error free coordinates and crystallographic R factor lower than 0.10, while polymer and powder structures were excluded. *p*-cymene ligands were considered forming stacking interaction if the angle between the mean planes of their aromatic rings was less than 10° and the centres of the rings belong to the ellipse defined by the horizontal displacement (offset) of 7.5 Å and normal distance

[a] University of Belgrade, Faculty of Chemistry, Studentski trg 12-16, 11000 Belgrade, Serbia, e-mail: szaric@chem.bg.ac.rs
[b] Department of Chemistry, Texas A&M University at Qatar, P.O. Box 23874, Doha, Qatar.

Electronic Supplementary Information (ESI) available: vibrational frequencies and intensities of optimized ruthenium complexes with p-cymene and benzene. See DOI: 10.1039/x0xx00000x

of 6.0 Å, with the ellipse centre being the centre of one of the rings (Figure 1).

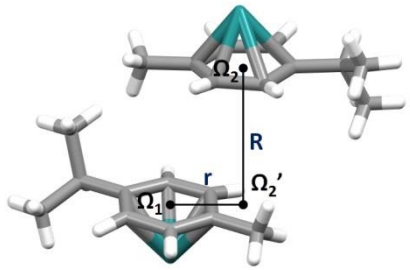

Figure 1. Model system for CSD search of stacking interactions between *p*-cymene ligands. Ω_1 and Ω_2 are centres of aromatic rings of *p*-cymene ligands, while Ω_2' is the projection of centre Ω_2 onto the plane of aromatic ring of Ω_1. Normal distance R is the distance from Ω_2 to Ω_2', while horizontal displacement or offset is the distance from Ω_1 to Ω_2'.

We have used several additional parameters to determine the mutual orientation of *p*-cymene ligands. Torsion angle T was used to determine the orientation of methyl groups of isopropyl substituent of one *p*-cymene relative to the aromatic ring of the other *p*-cymene (Figures 2a). Torsion angle T' was used to determine the mutual orientation of *p*-cymene substituents (Figures 2b).

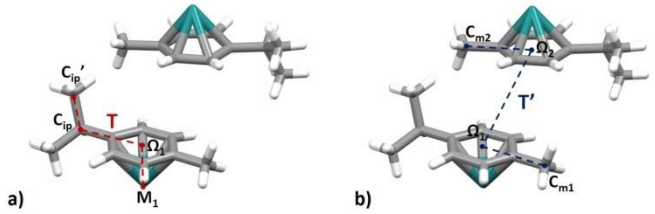

Figure 2. a) Torsion angle T is defined as the absolute value of torsion C_{ip}'-C_{ip}-Ω_1-M_1, where C_{ip} is the 3° and C_{ip} is the 1° carbon of isopropyl substituent. Since there are two 1° carbon atoms and therefore two torsion angles of this type, torsion T is the one with the larger value; b) torsion angle T' is defined as the absolute value of torsion C_{m1}-Ω_1-Ω_2-C_{m2}, where C_{m1} and C_{m2} are methyl substituents of *p*-cymene ligands.

In order to determine the strength of the interactions between *p*-cymene ligands, quantum chemical calculations were performed on [Ru(*p*-cym)$Cl_2(NH_3)$] complex, since the vast majority of the complexes found in crystal structures were of ruthenium, with chloride and nitrogen ligands. This complex was optimized using the B97 density functional[33] with D2 dispersion correction by Grimme[33] and def2-TZVP basis set,[34] using the effective core potentials for ruthenium.[35] The same level of theory was used for the calculations of stacking interaction energies between two of these complexes, which included the BSSE removal according to the counterpoise procedure.[36] This level was used since it was previously shown to give good results on interactions between uncoordinated benzene and benzene coordinated to ruthenium.[29] Electrostatic potential map of the [Ru(*p*-cym)$Cl_2(NH_3)$] molecule was also calculated at B97-D2/def2-TZVP level. It was mapped on the surface defined by the electron density of 0.004 a.u.[37] In order to estimate the influence of substituents on the interaction energies, additional calculations were performed on dimer of [Ru(benzene)$Cl_2(NH_3)$] complex, using the same level of theory. All calculations were performed in Gaussian 09 (version D.01) program package.[38]

Results and discussion

Cambridge Structural Database Search

The CSD search gave a total of 679 stacking interactions between *p*-cymene ligands satisfying the given geometrical criteria. As expected, the vast majority of these interactions (612, or 90.1%) was between *p*-cymene ruthenium complexes, since *p*-cymene is a typical ligand for ruthenium; the ruthenium complexes were mostly of half-sandwich type (576, or 94.1%), which is also typical for *p*-cymene organometallic compounds. The rest of the complexes were with osmium.

In the 617 of structures with stacking interactions (or 90.9%) the torsion angle T has values larger than 150° (Figure 3a), which indicates that one methyl group of isopropyl substituent of *p*-cymene has tendency to be pointed towards the plane of aromatic ring of the other *p*-cymene. Vast majority of the stacking interactions (660, or 97.2%) has torsion angle T' in the range 170-180° (Figure 3b), which indicated preference for antiparallel orientation of *p*-cymene ligands. Further analysis of stacking interactions in crystal structures was therefore conducted on contacts with antiparallel orientation.

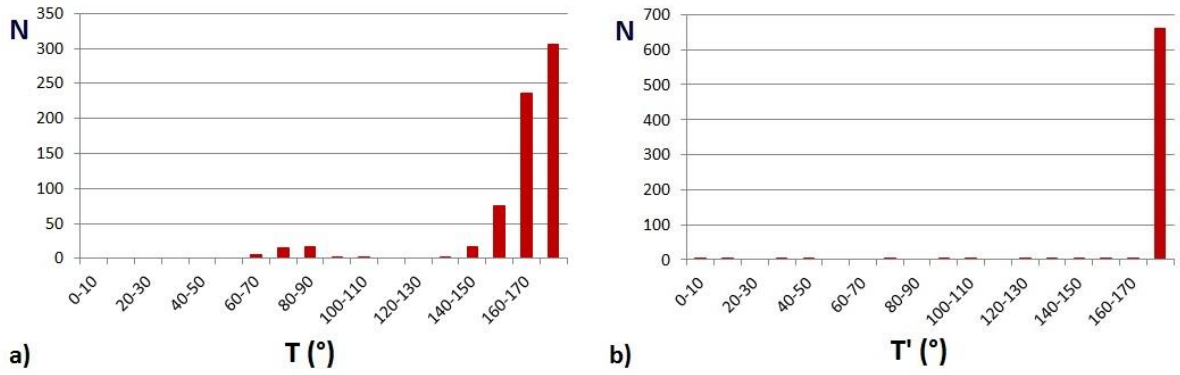

Figure 3. Distributions of torsion angles T (a) and T' (b). The angles are described at Figure 2.

In order to obtain the mutual orientation of antiparallel *p*-cymene ligands, offsets for all the contacts were decomposed into horizontal and vertical component (r_x and r_y, Figure 4). The obtained density map has three highly populated areas (Figure 4), indicating preference for three stacking geometries.

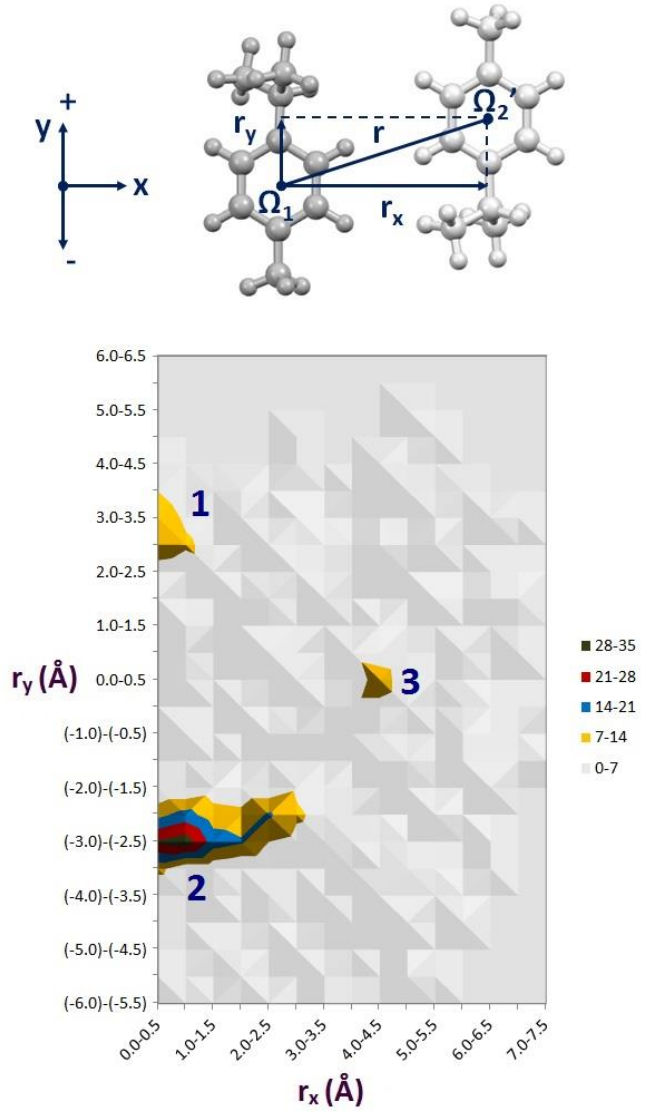

Figure 4. Density map of horizontal (r_x) and vertical (r_y) component of offset values for stacking interactions between *p*-cymene ligands found in CSD crystal structures.

The first area on the map (1, Figure 4) has r_x = 0.0 – 0.5 Å and r_y = 2.5 – 3.0 Å and normal distances R = 4.5 – 5.0 (Figure 5), which indicates the displacement along the substituents of aromatic ring, with isopropyl group of one *p*-cymene above the aromatic ring of the other *p*-cymene, and vice versa. The example of type 1 geometry was found in the crystal structure of (N-(2-Aminoethyl)methanesulfonamidato)-chloro-(η^6-1*p*-cymene)-ruthenium(II) (refcode UDUDOO, Figure 6).[39] Since the majority of the structures has large values of torsion angle T (Figure 3), one methyl group of isopropyl substituent of each *p*-cymene is pointed towards the aromatic ring of the other *p*-cymene forming two C-H/π interactions, and, consequently, very large normal distances, which probably lowers the strength of stacking between aromatic rings.

The area on the map denoted as 2 (Figure 4) is the most populated one. The largest number of geometries belonging to this area are with r_x = 0.0 – 0.5 Å and r_y = (-3.0) – (-2.5) Å (Figure 4) and normal distances R ≈ 3.5 Å (Figure 5). These values indicate that *p*-cymene ligands are displaced along the substituents of aromatic ring, with methyl substituent of one *p*-cymene above the aromatic ring of the other *p*-cymene, and vice versa. These methyl substituents form C-H/π interactions, which support the stacking of aromatic rings, which should be substantial at these normal distances. The example of type 2 geometry was found in the crystal structure of (η^6-*p*-cymene)-(N-methoxycarbonylmethyl-α,N-didehydroalaninato-O,N)-chloro-ruthenium(II) (refcode YIXNOI, Figure 6).[40]

The populated area 3 (Figure 4) and the geometries this area represents have r_x = 4.0 – 4.5 Å and r_y = 0.0 – 0.5 Å (Figure 4), with normal distances of R = 2.5 – 3.0 Å (Figure 5). These parameters indicate the displacement along the line normal to the substituents, and stacking interaction with large horizontal displacement is formed. Additionally, substituents of aromatic rings interact with each other, as well with edges of aromatic rings. The example of this geometry was found in the crystal structure of chloro-(η^6-*p*-cymene)-(2-methyl-N-((1H-pyrrol-2-yl)methyl)propan-2-aminato)-ruthenium(II) (refcode PUJYEA, Figure 6).[27]

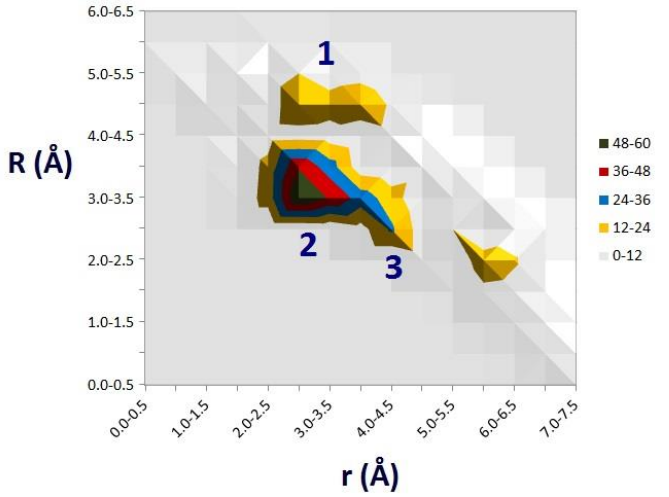

Figure 5. Density map of normal distance (R) versus horizontal displacement (r) for stacking interactions between *p*-cymene ligands found in CSD crystal structures

Quantum Chemical Calculations

In order to explain the tendencies towards certain stacking geometries found in the CSD crystal structures, we have performed the calculations of interaction energies between complexes with *p*-cymene ligands. Since we determined that the vast majority of the interacting *p*-cymene complexes from the CSD are ruthenium(II) complexes with chloride and nitrogen ligands, model molecule for the calculations was [Ru(*p*-cym)Cl_2(NH_3)]. The geometry of this molecule optimized at B97-D2/def2-TZVP level of theory has the absolute value of

torsion angle T of 174.71°, which is in agreement with the values of this angle in the CSD crystal structures (Figure 3).

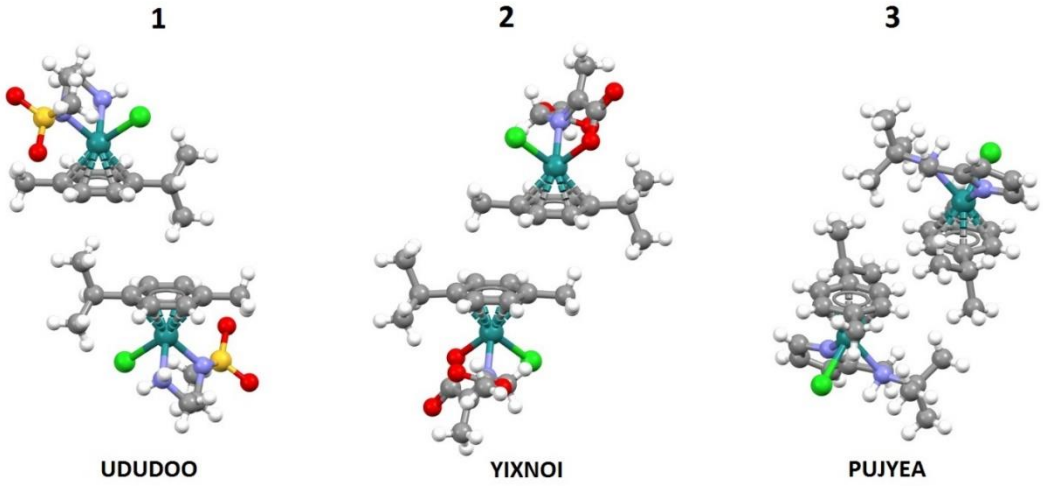

Figure 6. Three typical geometries of stacking interactions between *p*-cymene ligands. The numbers above them indicate the position of the geometry on the offset density maps (Figures 4 and 5), while the letters below indicate their CSD refcode.

Starting from the sandwich orientation of aromatic rings, the *p*-cymene-containing ruthenium complexes were displaced along the substituents (model system Y, Figure 7) and along the line normal to the substituents (model system X, Figure 8). For the model system Y we have distinguished the positive offsets (isopropyl substituents getting closer) and negative offsets (methyl substituents getting closer, Figure 7). In a series of single point B97-D2/def2-TZVP calculations, we have kept the monomer geometries rigid and for certain offset values we have changed the normal distances in order to find the ones with the strongest interactions. The results of the calculations are presented in Figures 7 and 8 as potential energy curves.

Potential energy curve for model system Y shows two minima. More stable minimum has horizontal displacement of -2.5 Å and normal distance of 3.4 Å (Figure 7), which corresponds to the most frequent interaction geometry found in crystal structures (2, Figures 4-6). The frequency of this geometry can therefore be explained by the fact that this is the most stable interaction between *p*-cymene complexes we have calculated, with interaction energy of -7.56 kcal/mol. In order to assess how much the substituents are strengthening the interactions, interaction energies were also calculated between [Ru(benzene)$Cl_2(NH_3)$] complexes, keeping the offset and optimal normal distances between *p*-cymene complexes (r = -2.5 Å ad R = 3.4 Å). The interaction energy for stacking between benzene complexes, is -3.93 kcal/mol, which implies that substituents are strengthening the overall interaction almost twice by forming two C-H/π interactions. Therefore it can be said that in the geometry of type 2 the overall interaction is a combination of π-π stacking and C-H/π interactions.

It is interesting to notice that the stacking energy between [Ru(benzene)$Cl_2(NH_3)$] molecules at 2.5 Å is -3.93 kcal/mol, while our previously calculated stacking energy at the same offset between two Cr-benzene half-sandwich compounds [Cr(benzene)$(CO)_3$] is -3.11 kcal/mol and between two Cr-benzene sandwich compounds [Cr(benzene)$_2$] is -3.63 kcal/mol.[18] This is in agreement with the calculations by Merino et al. that showed that aromatic rings coordinated to 4d metals stack stronger than aromatic rings coordinated to 3d metals.[20]

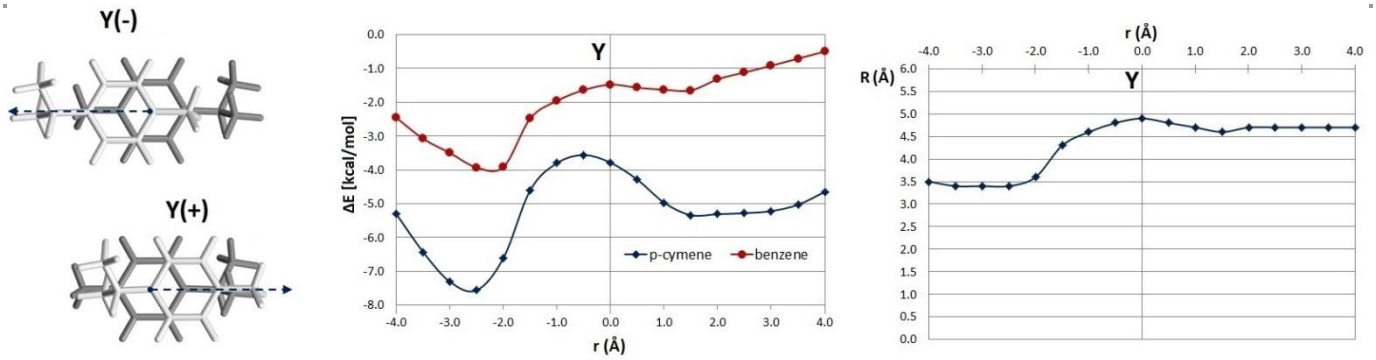

Figure 7. Model system Y (left) for calculations of stacking interaction energies between two *p*-cymene ligands in [Ru(*p*-cym)$Cl_2(NH_3)$] (for the reasons of simplicity, only *p*-cymene ligands are shown). Potential energy curves (middle) were calculated at B97-D2/def2-TZVP level of theory, using the effective core potentials for ruthenium atoms, and they represent the energies of the strongest interactions at given offsets. For the same optimal normal distances (right), interaction energies between two [Ru(benzene)$Cl_2(NH_3)$] complexes were calculated (middle).

The other minimum on Y potential energy curve has horizontal displacement of 1.5 Å, with interaction energy of -5.34 kcal/mol. However, interaction energies are very similar for displacements between 2.0 and 3.5 Å as well (between -5.03 and -5.31 kcal/mol, Figure 7); optimal normal distances for these offsets are 4.6-4.7 Å. This area on the curve therefore corresponds to the second most frequent geometry found in crystal structures (1, Figures 4-6). The effect of the substituents in this geometry is quite large. Namely, if *p*-cymene ligand is replaced with benzene, the stacking between complexes is significantly weaker; interactions are weaker than -1.5 kcal/mol for the offsets between 2.0 and 3.5 Å (Figure 7), since normal distances between the rings are quite large due to C-H/π interactions of methyl groups of isopropyl substituents and aromatic rings. It can be sad that isopropyl substituents quite significantly strengthen the overall interaction in type 1 structures, which are therefore dominated by the C-H/π interactions, while stacking is only a minor stabilizing effect.

Potential energy curve for model system X has a minimum at larger horizontal displacement of 3.5 Å (Figure 8), with the optimal normal distance of 3.1 Å and interaction energy of -6.14 kcal/mol. This minimum has very similar geometry as the third most frequent interaction type in crystal structures (3, Figures 4-6). The interaction energy between corresponding benzene complexes in this geometry is -3.10 kcal/mol (Figure 8), which suggests that substituents are strengthening the overall interaction at least twice by their mutual interactions and by interacting with edges of aromatic rings.

The preferred interaction geometries between *p*-cymene ligands can be explained by observing the electrostatic potential map of [Ru(*p*-cym)$Cl_2(NH_3)$]. The map shows that potentials are slightly negative above aromatic ring, positive at the aromatic edges, and positive at the hydrogen atoms of methyl groups (Figure 9). Therefore, it can be said that the geometries of types 1 and 2 (Figures 6) are consequences of overlaying of positive potentials of methyl hydrogens and negative potentials above aromatic rings (Figure 9). The geometry of type 3 (Figures 6) is the consequence of overlaying of negative potential above aromatic ring of one *p*-cymene and positive potential at the aromatic edges of the other *p*-cymene, and vice versa (Figure 9).

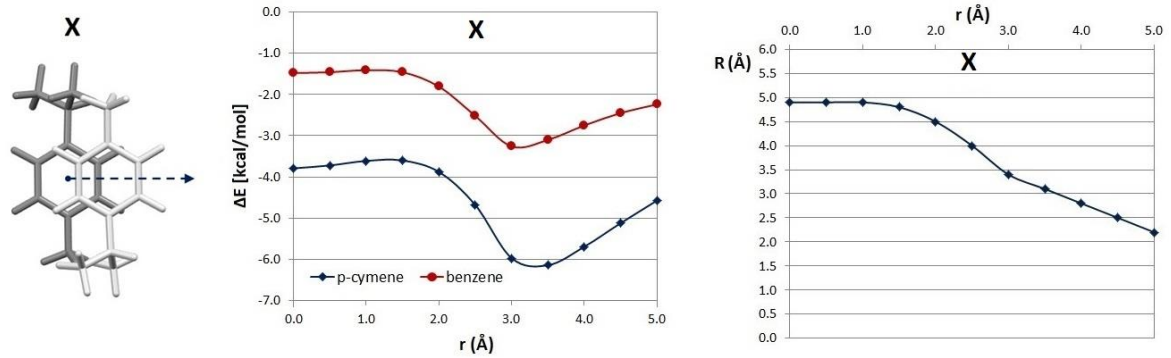

Figure 8. Model system X (left) for calculations of stacking interaction energies between two *p*-cymene ligands in [Ru(*p*-cym)$Cl_2(NH_3)$] (for the reasons of simplicity, only *p*-cymene ligands are shown). Potential energy curves (middle) were calculated at B97-D2/def2-TZVP level of theory, using the effective core potentials for ruthenium atoms, and they represent the energies of the strongest interactions at given offsets. For the same optimal normal distances (right), interaction energies between two [Ru(benzene)$Cl_2(NH_3)$] complexes were calculated (middle).

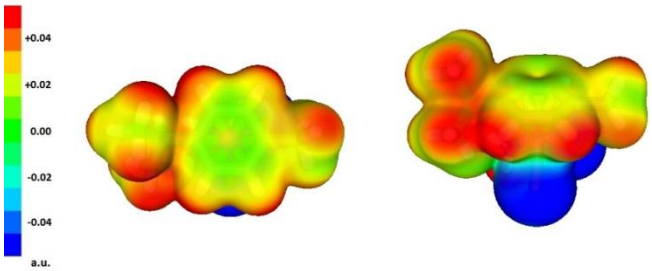

Figure 9. Upper and side views of the electrostatic potential map of [Ru(*p*-cym)$Cl_2(NH_3)$]. The potentials were mapped on the surface defined by the electron density of 0.004 a.u. using the B97-D2/def2-TZVP Gaussian wave functions.

Conclusions

Stacking interactions between *p*-cymene ligands of transition metal complexes were studied by searching the crystal structures deposited in the Cambridge Structural Database and by performing DFT calculations. The CSD search found three preferred interaction geometries between coordinated *p*-cymenes, which were majorly ligands in ruthenium half-sandwich compounds with chloride and nitrogen ligands. The most frequent interaction geometry had stacking interaction between aromatic rings, as well as two C-H/π interactions between methyl substituents and aromatic rings. The second geometry had stacking between aromatic rings and two C-H/π interactions between aromatic rings and methyl groups of isopropyl substituents, while the third one included stacking at large offsets (around 4.0 Å), as well as interactions between substituents and between substituents and aromatic ring edges.

DFT calculations of interaction energies on model complex [Ru(*p*-cym)$Cl_2(NH_3)$] showed that the geometries derived from the CSD crystal structures are so frequent because they all correspond to potential energy curve minima. The strongest interaction was calculated for the geometry corresponding to

the most frequent one in the CSD, with B97-D2/def2-TZVP interaction energy of -7.56 kcal/mol. The energy of interaction between benzene ligands in [Ru(benzene)$Cl_2(NH_3)$] for the same geometrical parameters is -3.93 kcal/mol, which implies that methyl substituents of *p*-cymene rings strengthen the stacking interaction twice by forming two C-H/π interactions with aromatic rings. This effect is even more pronounced if methyl groups of isopropyl substituents interact with aromatic rings, since their C-H/π interactions can strengthen the stacking five times.

The preference for certain interaction geometries can be explained by observing the electrostatic potential surface of [Ru(*p*-cym)$Cl_2(NH_3)$] complex, which is negative above aromatic ring and positive at the ring edges and at hydrogen atoms of methyl groups.

This work shows that the presence of substituents on coordinated aromatic rings can lead to large changes in the geometries of stacking interactions and can significantly strengthen the overall interactions by providing additional contacts with aromatic rings.

Conflicts of interest

There are no conflicts to declare.

Acknowledgements

This work was funded by the Ministry of Education, Science and Technological Development of the Republic of Serbia (grant 172065). The authors would like to thank the IT Research Computing Group at Texas A&M University at Qatar, which is funded by the Qatar Foundation for Education, Science and Community Development, for providing the high-performance computing resources used in this work.

Notes and references

1 L. M. Salonen, M. Ellermann and F. Diederich, *Angew. Chemie - Int. Ed.*, 2011, **50**, 4808–4842.
2 T. Chen, M. Li and J. Liu, *Cryst. Growth Des.*, 2018, **18**, 2765–2783.
3 V. L. Malinovskii, F. Samain and R. Häner, *Angew. Chemie Int. Ed.*, 2007, **46**, 4464–4467.
4 C. A. Hunter and J. K. M. Sanders, *J. Am. Chem. Soc.*, 1990, **112**, 5525–5534.
5 S. Balakrishnan and S. P. Sarma, *Biochemistry*, 2017, **56**, 4346–4359.
6 Q. Hou, R. Bourgeas, F. Pucci and M. Rooman, *Sci. Rep.*, 2018, **8**, 14661.
7 E. Ahmed, D. P. Karothu and P. Naumov, *Angew. Chemie Int. Ed.*, 2018, **57**, 8837–8846.
8 D. P. Malenov, G. V. Janjić, V. B. Medaković, M. B. Hall and S. D. Zarić, *Coord. Chem. Rev.*, 2017, **345**, 318–341.
9 W.-R. Zhuang, Y. Wang, P.-F. Cui, L. Xing, J. Lee, D. Kim, H.-L. Jiang and Y.-K. Oh, *J. Control. Release*, 2019, **294**, 311–326.
10 E. C. Lee, D. Kim, P. Jurečka, P. Tarakeshwar, P. Hobza and K. S. Kim, *J. Phys. Chem. A*, 2007, **111**, 3446–3457.
11 O. Bludský, M. Rubeš, P. Soldán and P. Nachtigall, *J. Chem. Phys.*, 2008, **128**, 114102.
12 D. B. Ninković, G. V. Janjić, D. Ž. Veljković, D. N. Sredojević and S. D. Zarić, *ChemPhysChem*, 2011, **12**, 3511–3514.
13 J. P. Blagojević and S. D. Zarić, *Chem. Commun.*, 2015, **51**, 12989–12991.
14 D. P. Malenov and S. D. Zarić, *Dalton Trans.*, 2019, **48**, 6328–6332.
15 D. P. Malenov, M. B. Hall and S. D. Zarić, *Int. J. Quantum Chem.*, 2018, **118**, e25629.
16 D. P. Malenov and S. D. Zarić, *Phys. Chem. Chem. Phys.*, 2018, **20**, 14053–14060.
17 S. T. Mutter and J. A. Platts, *Chem. - A Eur. J.*, 2010, **16**, 5391–5399.
18 D. P. Malenov, I. S. Antonijević, M. B. Hall and S. D. Zarić, *CrystEngComm*, 2018, **20**, 4506–4514.
19 D. P. Malenov, J. L. Dragelj, G. V. Janjić and S. D. Zarić, *Cryst. Growth Des.*, 2016, **16**, 4169–4172.
20 A. Vargas-Caamal, S. Pan, F. Ortiz-Chi, J. L. Cabellos, R. A. Boto, J. Contreras-Garcia, A. Restrepo, P. K. Chattaraj and G. Merino, *Phys. Chem. Chem. Phys.*, 2016, **18**, 550–556.
21 M. O. Sinnokrot and C. D. Sherrill, *J. Phys. Chem. A*, 2003, 107, 8377–8379.
22 S. E. Wheeler and K. N. Houk, *J. Am. Chem. Soc.*, 2008, **130**, 10854–10855.
23 S. E. Wheeler, *J. Am. Chem. Soc.*, 2011, **133**, 10262–10274.
24 S. E. Wheeler, *Acc. Chem. Res.*, 2013, **46**, 1029–1038.
25 F. Wang, H. Chen, S. Parsons, I. D. H. Oswald, J. E. Davidson and P. J. Sadler, *Chem. - A Eur. J.*, 2003, **9**, 5810–5820.
26 H. Chen, J. A. Parkinson, S. Parsons, R. A. Coxall, R. O. Gould and P. J. Sadler, *J. Am. Chem. Soc.*, 2002, **124**, 3064–3082.
27 Y.-H. Chang, W.-J. Leu, A. Datta, H.-C. Hsiao, C.-H. Lin, J.-H. Guh and J.-H. Huang, *Dalton Trans.*, 2015, **44**, 16107–16118.
28 M. Formánek and J. V. Burda, *Chem. Phys. Lett.*, 2014, **598**, 28–34.
29 S. T. Mutter and J. A. Platts, *J. Phys. Chem. A*, 2011, **115**, 11293–11302.
30 Y. K. Yan, M. Melchart, A. Habtemariam, A. F. A. Peacock and P. J. Sadler, *JBIC J. Biol. Inorg. Chem.*, 2006, **11**, 483–488.
31 C. R. Groom, I. J. Bruno, M. P. Lightfoot and S. C. Ward, *Acta Crystallogr. Sect. B Struct. Sci. Cryst. Eng. Mater.*, 2016, **72**, 171–179.
32 I. J. Bruno, J. C. Cole, P. R. Edgington, M. Kessler, C. F. Macrae, P. McCabe, J. Pearson, R. Taylor and IUCr, *Acta Crystallogr. Sect. B Struct. Sci.*, 2002, **58**, 389–397.
33 S. Grimme, *J. Comput. Chem.*, 2006, **27**, 1787–1799.
34 F. Weigend and R. Ahlrichs, *Phys. Chem. Chem. Phys.*, 2005, **7**, 3297–305.
35 D. Andrae, U. Häußermann, M. Dolg, H. Stoll and H. Preuß, *Theor. Chim. Acta*, 1990, **77**, 123–141.
36 S. Boys and F. Bernardi, *Mol. Phys.*, 1970, **19**, 553–566.
37 J. S. Murray, Z. P.-I. Shields, P. Lane, L. Macaveiu and F. A. Bulat, *J. Mol. Model.*, 2013, **19**, 2825–2833.
38 M. J. Frisch, G. W. Trucks, H. B. Schlegel, G. E. Scuseria, M. A. Robb, J. R. Cheeseman, G. Scalmani, V. Barone, G. A. Petersson, H. Nakatsuji, X. Li, M. Caricato, A. Marenich, J. Bloino, B. G. Janesko, R. Gomperts, B. Mennucci, H. P. Hratchian, J. V. Ortiz, A. F. Izmaylov, J. L. Sonnenberg, D. Williams-Young, F. Ding, F. Lipparini, F. Egidi, J. Goings, B. Peng, A. Petrone, T. Henderson, D. Ranasinghe, V. G. Zakrzewski, J. Gao, N. Rega, G. Zheng, W. Liang, M. Hada, M. Ehara, K. Toyota, R. Fukuda, J. Hasegawa, M. Ishida, T. Nakajima, Y. Honda, O. Kitao, H. Nakai, T. Vreven, K. Throssell, J. A. Montgomery Jr., J. E. Peralta, F. Ogliaro, M. Bearpark, J. J. Heyd, E. Brothers, K. N. Kudin, V. N. Staroverov, T. Keith, R. Kobayashi, J. Normand, K. Raghavachari, A. Rendell, J. C. Burant, S. S. Iyengar, J. Tomasi, M. Cossi, J. M. Millam, M. Klene, C. Adamo, R. Cammi, J. W. Ochterski, R. L. Martin, K. Morokuma, O. Farkas, J. B. Foresman and D. J. Fox, *Gaussian 09, Revis. D.01*, 2016.

39 J. J. Soldevila-Barreda, P. C. A. Bruijnincx, A. Habtemariam, G. J. Clarkson, R. J. Deeth and P. J. Sadler, *Organometallics*, 2012, **31**, 5958–5967.
40 K. Severin, R. Bergs, M. Maurus, S. Mihan and W. Beck, *Zeitschrift für Naturforsch. B*, 1995, **50**, 265–274.